Advantages of nanoscale bioactive glass as inorganic filler in alginate hydrogels for drug delivery and biofabrication

Journal Article

Author(s):
Bider, Faina; Karakaya, Emine; Mohn, Dirk ⓘ; Boccaccini, Aldo R.
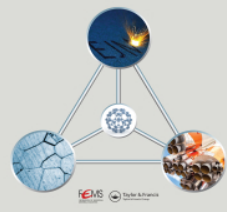
Advantages of nanoscale bioactive glass as inorganic filler in alginate hydrogels for drug delivery and biofabrication

Faina Bider, Emine Karakaya, Dirk Mohn, Aldo R. & Boccaccini

Routledge
Taylor & Francis Group

Advantages of nanoscale bioactive glass as inorganic filler in alginate hydrogels for drug delivery and biofabrication

Faina Bider[a], Emine Karakaya[a], Dirk Mohn[b,c], and Aldo R. Boccaccini[a]

[a]Institute of Biomaterials, University of Erlangen-Nuremberg, Erlangen, Germany; [b]Clinic of Conservative and Preventive Dentistry, Center for Dental Medicine, University of Zurich, Zurich, Switzerland; [c]Institute for Chemical and Bioengineering, Department of Chemistry and Applied Biosciences, ETH Zurich, Zurich, Switzerland

ABSTRACT

Sodium alginate is a natural biocompatible polymer obtained from brown algae which has found numerous biomedical applications. Inorganic fillers, such as nanosized bioactive glass (nBG) particles, are well known for their outstanding properties in terms of being osteoconductive and osteoinductive and therefore finding application in bone tissue engineering. In this study, the impact of nBG particles on alginate hydrogels was investigated for applications of the composite hydrogel in biofabrication and drug delivery. The influence of nBG particles on properties such as printability, drug release ability and bioactivity (capability to form a hydroxyapatite (HAp) layer on the surface of nBG-alginate capsules) was studied. In vitro cell studies proved high cell viability of all inks. Due to the presence of nBG particles, more precise printed grids and pore sizes were achieved. Moreover, a decrease of the release of the model drug icariin in the presence of nBG particles was determined. The formation of a HAp layer on the surface of nBG-alginate capsules was assessed by FTIR, XRD and SEM. Overall, the addition of nBG particles into alginate hydrogels led to the improvement of the relevant properties investigated. Therefore, nBG-alginate systems should gain more attention for 3D bioprinting and drug delivery approaches.

CONTACT Aldo R. Boccaccini ✉ aldo.boccaccini@fau.de 🖅 Institute of Biomaterials, University of Erlangen-Nuremberg, Erlangen, Germany.

1. Introduction

Tissue engineering (TE) has the aim to develop tissue substitutes combining biomaterials with signalling molecules and cells to mimic the functions of human organs (Chen & Liu, 2016; Khademhosseini, Vacanti, & Langer, 2009; Khademhosseini & Langer, 2016). One important branch of TE concerns bone regeneration (Salgado, Coutinho, & Reis, 2004; Vallet-Regí, 2006). Sodium alginate, a marine-derived natural polymer obtained from brown algae, is one of the most widely used polysaccharides in the biomedical field and has numerous advantages for applications in drug delivery systems and TE scaffolds (Draget, Skjåk-Braek, & Smidsrød, 1997; Rastin et al., 2020; Tønnesen & Karlsen, 2002). Alginate based hydrogels have been investigated also extensively in the field of cell encapsulation (Ghidoni et al., 2008; Tan & Takeuchi, 2007). In such hydrogel systems, the surrounding 3 D-network of suitable stiffness allows an exchange of oxygen and nutrients for encapsulated cells and provides an optimal environment for cell growth (Frampton, Hynd, Shuler, & Shain, 2011). Furthermore, alginate provides various mild crosslinking options and further chemical modifications are possible to achieve improved biocompatibility (Orive, Carcaboso, Hernández, Gascón, & Pedraz, 2005).

Bioactive glasses (BGs), a family of bioreactive inorganic materials, are highly investigated biomaterials in bone tissue engineering due to their outstanding features, e.g. regulation of cell behavior via the release of biologically active ions, osteoconductivity and osteoinductivity (Leite et al., 2016; Xynos, Edgar, Buttery, Hench, & Polak, 2001). For this reason, recently, increasing attention has been paid to the development of composites by incorporation of BGs in suitable hydrogels, which are proposed for applications in TE (Venkatesan, Bhatnagar, Manivasagan, Kang, & Kim, 2015). In general, polymers and inorganic fillers can be combined to achieve composite systems exploiting the relative advantages of both materials. For example, bioactive inorganic fillers, such as 45S5 BG, are investigated as convenient fillers in alginate to improve the properties of this hydrogel for bone regeneration applications, particularly to influence the mineralisation process and osteoinductive properties (Zeng, Han, Li, & Chang, 2014).

The main aim of this study was to determine the impact of BG nanoparticles on the properties of alginate based composite hydrogels. Thus, a small amount of nanosized bioactive glass (nBG) particles was incorporated in alginate to obtain a composite material which was investigated in terms of formation of microcapsules, drug release, bioactivity, printability (in the context of biofabrication), as well as cell compatibility. The ability of the system to incorporate and release a therapeutic drug,

in this case the plant derived icariin, was also discussed. Icariin is a natural based drug which is extracted from Epimedium species and is known for the promotion of osteoblast cells and the inhibition of osteoclast cells, being species thus relevant for the intended applications in bone tissue engineering (Shen et al., 2020; Zhang, Liu, Huang, Wismeijer, & Liu, 2014; Zhao et al., 2010). The present study differs from our previous work (Leite et al., 2016) in that here nBG synthesized by flame spraying technology (and not sol-gel derived BG particles) were used and microcapsules were developed. In addition, we investigated the release of a natural drug in contrast to a synthetic drug (ibuprofen) used in the previous study (Leite et al., 2016).

2. Materials and methods

2.1. Materials

Alginate (alginic acid sodium salt from marine brown algae, Vivapharm, Germany), Hank's Balanced Salt Solution (HBSS); Dulbeccós Phosphate Buffered Saline (DPBS, [-] Ca^{2+}, [-] Mg^{2+}), Phosphate buffer saline (PBS, Gibco), calcein AM and 4′,6-Diamidin-2-phenylindol (DAPI), Dulbeccós Modified Eagle Medium (DMEM, 4.5 g/L D-Glucose, Pyruvate), L-Glutamine, were obtained from ThermoFisher, Invitrogen (Germany). Calcium chloride ($CaCl_2$) was purchased from Sigma Aldrich (Germany). Icariin was obtained from Changsha Herbway Biotech Co. Ltd (China). nBG particles were received from ETH Zurich (Switzerland) and were obtained through flame spray synthesis, following the protocol of Brunner et. al (Brunner, Grass, & Stark, 2006). Briefly, via mixing the corresponding liquid metallic precursors and injecting the liquid mixture into a flame reactor the nanoparticles are produced. Subsequently, the nano sized powder is collected on a filter located above the flame. The size of the nBG particles used in this study was in the range 20-60 nm. The composition is shown in Table 1, which is close to the standard 45S5 BG composition (Xynos et al., 2001). The same nBG has been used in previous investigations to develop composites, e.g. in combination with poly(3hydroxybutyrate) (P(3HB)), polyisoprene (PI), polycaprolactone (PCL) or alginate dialdehyde/gelatin systems (see for example (Mohn et al., 2010)).

Table 1. The chemical composition (wt%) of nBG particles investigated in the current study and the respective BET-specific surface area (SSA).

	SiO_2	Na_2O	CaO	P_2O_5	SSA (m^2g^{-1})
n-BG	47.8	25.1	22.6	4.6	35

2.2. Capsules fabrication

1% (w/v) alginate was dissolved in HBSS at room temperature (RT). For alginate-nBG capsules 0.1% (w/v) n-BG power was added into pure alginate hydrogel and sonicated for 1 hour in total using a sonication device (Ultrasonic Homogenizers, Germany), alternating different periods of continuous stirring to ensure a homogeneous nBG dispersion. The process involved placing the samples into the US bath for 15 min, subsequently stirring for 15 min, and placing it again 15 min in the US bath followed by a final 15 min stirring. The entire process lasted for 1 h.

For the drug release study, additionally 0.1% (w/v) of icariin solution was added to the alginate and alginate-nBG solution for further 10 min. The icariin solution was made of grinded icariin powder which was also dissolved in HBSS for several hours at 37 °C. The icariin concentration in HBSS was 0.1% (w/v).

The manufacturing of the microcapsules was conducted using a commercially available encapsulator (B-390, Büchi, Switzerland) and a syringe pump (type AL-1000, World Precision Instruments, USA). The prepared mixtures were transferred into a 20 ml syringe, which itself was placed in the syringe pump and connected with the material intake of the encapsulator. Due to short time period (2 min) for the transferring step and for the extrusion process, no precipitation of nBG particles was observed. The encapsulator fabricated round hydrogel spheres by forcing the material through a 200 μm nozzle with a pulsation flow. The drops were collected in a beaker, which was placed on a stirring plate underneath the nozzle containing 0.1 M $CaCl_2$ solution to provide ionic cross-linking for 10 min. The capsules were collected in a cell strainer with 70 μm sized pores and washed with HBSS for further 10 min. After washing, the capsules (0.3 g per insert) were transferred to inserts which could suit into 6 well plates. Each well was filled with 3 ml of HBSS and incubated at 37 °C and 5.0% CO_2.

2.3. Capsule size measurement

A stereo microscope (Stemi 508, Carl Zeiss, Germany) was used to take images of icariin containing capsules with and without nBG after fabrication. 30 capsule images of each composition were measured to calculate the diameter using the ImageJ software (National Institutes of Health, USA). The mean diameter was calculated and evaluated to prove that an equal diameter range of all compositions had been achieved in order to be able to compare the release of icariin in drug release experiments.

2.4. Drug release study

In order to investigate the impact of nBG content on the release properties of the alginate capsules, icariin 0.1% (w/v) was added into alginate-nBG solution. The release of icariin out of pure alginate (reference) and alginate-nBG capsules was investigated by a UV-Vis spectrophotometer (Specord40, Analytic Jena, Germany) and analysed by WinASPECT 2.5.8.0 software. The characteristic absorption peak of icariin was determined at 277 nm. Briefly, 0.3 g of capsules containing icariin (with and without nBG) were placed into inserts, which were placed into 6 well-plates. Capsules were immersed in HBSS over 2 months (n = 3). At each time point (1, 3, 7, 14, 21, 28, 35, 42, 49 and 56 days) 1 ml of HBSS was removed for UV-Vis analysis, whereas 3 replicates were used. The stock solution of icariin was measured at day 0 and was characteristic for 100% release. The release of icariin (mg/ml) was obtained through the addition of the measured concentration of icariin at each time point. The calculation of drug release was performed by using the following equation:

$$dr_{\%} = \frac{m_x}{m_t} \times 100$$

where: $dr_{\%}$ is the percentage of drug release at each time point, m_x is the mean values of measured concentration with 3 replicas of icariin at each time point and m_t is the concentration of icariin in the stock solution.

2.5. Printability study

Alginate-nBG composite hydrogels were also investigated as inks for potential biofabrication approaches. Thus, to show the impact of nBG on printability properties of alginate hydrogels, a printability study over 7 days was performed. Printing was carried out on day 0 (time of preparation of inks) and on days 1, 3 and 7. For the 3 D printing process, a pneumatic 3 D printer (Bio X CELLINK BIO X, Boston, Massachusetts, USA) with a temperature controlled printerhead was used. Since 1% (w/v) alginate exhibits a too low viscosity for 3 D printing, 3% (w/v) alginate hydrogel with and without nBG was printed. After refilling 1% (w/v) alginate with and without nBG as well as 3% alginate with and without nBG a Filament Fusion test (resolution tree, see Figure S1, Supplementary Information) was printed at room temperature (RT) using
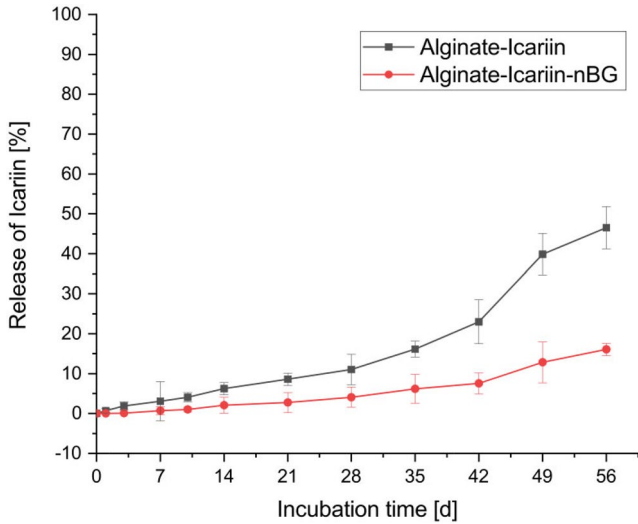
Figure 1. Release of icariin in HBSS from alginate and alginate-nBG capsules over 2 months.

printing pressures of 0-5 kPa for 1% alginate (w/v) and 60-70 kPa for 3% alginate (w/v) with a speed of 5 mm/sec. The resolution tree was generated with five different strut distances, ranging from 2.5 mm to 0.5 mm. Filament Fusion test (FFT) was performed with all 4 inks and on day 0. Furthermore, $10 \times 10 \times 3 \, mm^3$ samples were printed to show the possibility of printing overhanging structures. Overview images of the FFT and 3D structures were recorded with a camera and a stereomicroscope (Stemi 508, Zeiss, Germany) directly after printing. An overview of the developed inks and their associated investigated printing performances is shown in Table 2.

2.6. Bioactivity of capsules

In order to investigate the in vitro bioactivity of the capsules (e.g. their ability to develop in vitro hydroxyapatite crystals), capsules were immersed into a Simulated Body Fluid (SBF), which was prepared as described in the protocol of Kokubo et al. (Kokubo & Takadama, 2006). Alginate capsules with 0.1% nBG (w/v) particles were immersed in 25 ml of SBF (pH = 7.4) and were incubated at 37 °C and 120 rpm in a shaking incubator for 1, 3, 7, 14, 21 and 28 days. The SBF was changed two times a week to maintain a stable ion concentration. At each time point, the samples were removed from the SBF solution, washed with distilled water and dried in a freeze dryer and critical point dryer.

Table 2. Overview of investigated composite inks, printing performances and associated printing time points.

Inks	Filament Fusion Test	Timepoints	3D printed struts	Timepoints	Annotation
1% (w/v) alginate	X	Day 0	X	Day 0	Not considered due
1% (w/v) alginate + nBG	X	Day 0	X	Day 0-7	to low viscosity
3% (w/v) alginate	X	Day 0	X	Day 0	–
3% (w/v) alginate + nBG	X	Day 0	X	Day 0-7	–

2.7. Characterization of capsules

The capsules' chemical structure was investigated with FTIR, for which the samples were freeze dried. Different spectra were measured in absorption mode with a mean of 40 running scans at a $4\,cm^{-1}$ resolution.

XRD analysis was conducted to confirm hydroxyapatite (HAp) formation in nBG containing capsules immersed in SBF. CuK$_a$ radiation at 40 kV and 40 mA was utilized to achieve XRD patterns of grinded alginate-nBG capsules with 0.02° as a 2θ step in the 2θ range 20-80°.

SEM was performed to determine the possible formation of HAp on the surface of capsules after being immersed in SFB for over 4 weeks. To fix the alginate-nBG capsules two SEM fixing solution (each 1 hours) were used: SEM-Fix I, which is composed of 0.1% glutaraldehyde and 2% paraformaldehyde and SEM-Fix II, which is composed of 0.3% glutaraldehyde and 3% paraformaldehyde (both Sigma Aldrich, Germany). Afterwards an ethanol series until 99% ethanol for 30 min each was performed as preparation of the samples for the critical point drying process. Subsequently, the samples were dried by using a critical point dryer (EM CDP300, Leica) and thereafter they were fixed onto a carbon tape for SEM imaging.

2.8. In vitro characterization

To investigate the cell viability of the four inks, NIH/3T3 cells were embedded in 1% (w/v) and 3% (w/v) alginate with and without nBG and a live/dead staining was performed on day 0, 1, 3 and 7. Living cells were stained using calcein acetoxymethyl ester (calcein AM, Invitrogen, USA). After fixing the samples with 3.7% formaldehyde, a blue nucleic acid staining (4', 6-Diamidino-2-Phenylindole (DAPI), Invitrogen, USA) was performed to evaluate the total amount of cells. Subsequently, images were taken using a fluorescence microscope (Axio Scope A1, Carl Zeiss, Germany). The results were presented as average ± standard deviation. The cell viability was calculated according to the following equation:

$$Cell\ Viability\ [\%] = \frac{Surviving\ cells}{Total\ amount\ of\ cells} \times 100$$

2.9. Statistical analyses

Statistical analysis was performed via a one-way ANOVA test with the help of OriginLab (OriginLab 2019, USA) using the Bonferroni test as comparison of the mean values. The significance levels were set to $p < 0.05$ = *, $p < 0.01$ = ** and $p < 0.001$ = ***. $N = 3$ replicates were used for pore and grid size analysis and for the in vitro data.

3. Results and discussion

3.1. Drug release study

It is well known that alginate capsules provide successful drug carriers (Grassi, Colombo, & Lapasin, 2001). Alginate is well known for its ability to form carrier systems, e.g. membranes, films, microspheres, to deliver drugs (Jain & Bar-Shalom, 2014). Therefore, alginate was chosen in this work to encapsulate a plant-based drug, namely icariin, a phytotherapeutic compound investigated for its anti-cancer, antioxidant and antibacterial properties (Cao, Fu, & He, 2007). Moreover, icariin finds applications in bone tissue engineering due to its osteoinductive properties (Shen et al., 2020; Zhao et al., 2010; Zhang et al., 2014; Wu et al., 2009). The mentioned materials were dissolved in HBSS, which is a fluid salt solution (at physiological pH = 7) often used for solving processes.

To investigate the impact of nBG particles on the release ability of alginate hydrogels using icariin, a release study in HBSS was performed. Figure 1 shows the release of icariin out of pure alginate capsules and alginate-nBG capsules over 2 months. For both studies the capsule production was carried out using equal parameters. Yet, a non-significant difference between the capsule sizes with and without nBG particles was observed (Figure S2, Supplementary Information). Since the shape and diameters of capsules were non-significantly different, the release of icariin was comparable. The absorbance was measured at 277 nm and allowed a quantitative analysis about the total amount of icariin using a previously adjusted calibration curve. Subsequently, the icariin release was calculated in percent and plotted over time. It can be observed that the release of icariin from pure alginate capsules after 4 weeks is 11% ± 2, whereas the release out of nBG containing capsules was at 4% ± 2. After 8 weeks of incubation release values of 46% ± 5 without nBG and 16% ± 2 with nBG were measured.

Before the capsules were washed with HBSS and finally immersed into HBSS solution to observe the icariin release, they were crosslinked with 0.1 M CaCl$_2$ to induce capsule stability. The formation of capsules of pure alginate hydrogels occurs through M^{n+} ions, in this case Ca^{2+} ions (Bajpai & Sharma, 2004). This leads to an ionic interaction of Ca^{2+} ions with carboxylgroups (COO$^-$) mainly in G-units of alginate. Since the encapsulation process through 0.1 M CaCl$_2$ is mild, drugs can be released out of alginate capsules (Bajpai & Sharma, 2004). Bajpai et al. (Bajpai & Sharma, 2004) investigated the swelling and degradation behaviour of alginate capsules and observed that Ca^{2+} ions which are binding to -COO$^-$ units start to exchange with Na$^+$ ions from the external medium (Bajpai & Sharma, 2004). Therefore, the immersion of alginate capsules with and without nBG loaded with icariin into HBSS, which contains Na$^+$ ions, leads to a Ca^{2+} ion exchange in connection with COO$^-$ groups due to prior crosslinking with CaCl$_2$. Through Ca^{2+} ion diffusion out of the egg box structure of alginate into the surrounding HBSS, the capsules start to lose weight, degrade and slowly dissolve leading to a release of icariin into HBSS, which was measured with UV-Vis spectroscopy (Bajpai & Sharma, 2004). Therefore, on the one hand, icariin was released through the degradation of the carrier material (alginate), on the other hand, due to a diffusion processes. The diffusion rate is directly proportional to the G content of alginate hydrogel. Higher G-unit results in lower permeability of the hydrogel, which affects the drug release through diffusion (Banks, Enck, Wright, Opara, & Welker, 2019). In this study, alginate PH176 was used with a M-G ratio of 54%/46%. Due to the relative high amount of G-units and the relative slow degradation of alginate, the icariin release from pure alginate capsules can be explained. In case of nBG containing capsules, a significant reduced release of icariin was observed. It has been reported that apart from the external effect of Ca^{2+} to enable the crosslinking of alginate hydrogel, ionic dissolution of Ca^{2+} ions from nBG could lead to additional partial and slow in situ crosslinking with time (Han, Zeng, Li, & Chang, 2013). The icariin release deceleration in the case of nBG containing capsules is in agreement with this assumption.

3.2. Printability study

To investigate the impact of nBG particles on the printability properties of alginate, Filament Fusion tests (Figure 2a) and printing tests of 3 D structures (see Figure S3, Supplementary Information) were performed. The pores and grid size analysis of 3 D printed scaffolds is shown in Figure 2b and c. The Filament Fusion test was performed to visualize
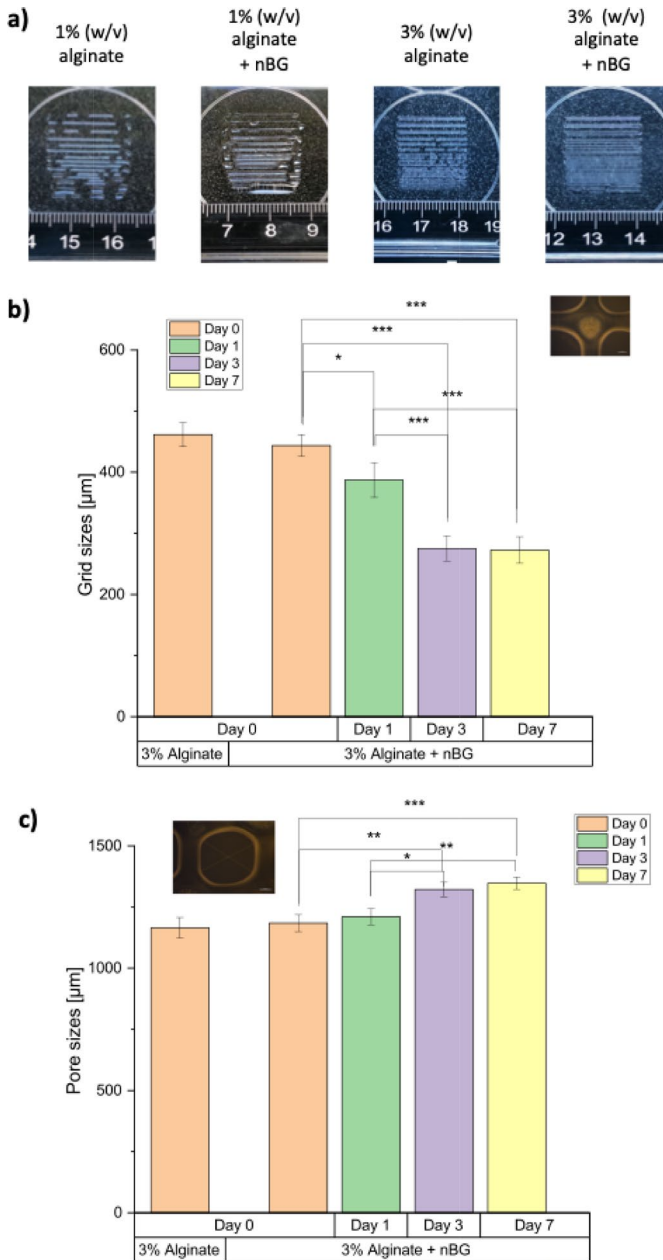
Figure 2. a) Results of printability test in terms of Filament Fusion Test with 1% and 3% (w/v) alginate with and without nBG particles. b) Grid sizes for 3% (w/v) alginate at day 0 and nBG containing hydrogel at days 0, 1, 3 and 7. c) Pore sizes of pure 3% (w/v) alginate at day 0 and nBG containing hydrogel at days 0, 1, 3 and 7. All data are displayed as mean ± SD. Statistical analysis was performed via a one-way ANOVA with the Bonferroni test for $p < 0.05 = *$, $p < 0.01 = **$ and $p < 0.001 = ***$.

Figure 3. SEM images of 1% (w/v) alginate capsules immersed in SBF for 14, 21, and 28 days and reference with 0.1% (w/v) nBG particles. Scale bar: 1 μm and 100 μm.
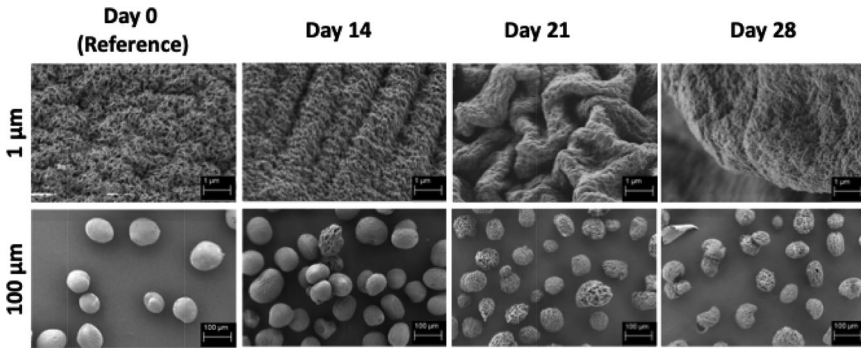
the effect of nBG particles on printing precision for two different polymer concentrations. It was observed that 1% (w/v) alginate ink with and without nBG exhibited no strut separation due to the low viscosity of this hydrogel. Therefore, it was not possible to create 3 D structures with such low concentrated alginate ink, even with added nBG. In regard to this assessment, a 3% (w/v) alginate concentration was chosen to investigate the ability to print 3 D structures. For 3% (w/v) alginate, it was observed that especially the addition of nBG particles led to better strut separations (lowest possible strut separation was 1.5 mm), whereas for nBG free 3% (w/v) alginate hydrogels especially the edges at the turning points were not as sharp as compared to those in structures printed with nBG containing hydrogel (lowest possible strut separation was 2 mm). 3 D structures with pure 3% (w/v) alginate hydrogel (without nBG particles) were also printed as a reference. Structures on day 1, 3 and 7 were printed only with nBG containing 3% (w/v) alginate ink to assess the impact of nBG particles. Figure 2b reveals a decreasing grid size with increasing printing time. Furthermore, increasing pore sizes (Figure 2c) 7 days after printing were observed. During the printing process the pressure parameter was kept constant at 60-70 kPa to be able to compare all printing results and to evaluate only the effect of nBG addition. The results indicate a possible impact of the presence of nBG particles on the improvement of the shape fidelity of 3 D printed structures.

Extrusion based printing is an additive manufacturing technique, which provides the opportunity to fabricate hydrogel scaffolds layer-by-layer (Ozbolat & Hospodiuk, 2016). However, the physical properties of the hydrogels in terms of concentration or molecular weight have a high impact on the viscosity and therefore on 3 D printed shape fidelity (Kong, Lee, & Mooney, 2002). In this study the concentration of alginate was increased up to 3% (w/v) to maintain shape fidelity during the printing

process. According to literature, nBG particles have an ability to release ions, e.g. Si and Ca ions, which can control the level of osteoblast bio-mineralization (Tousi et al., 2013). It is well known that alginate can crosslink in the presence of $CaCl_2$ (Bajpai & Sharma, 2004). During the printability test an additional crosslinking effect of Ca^{2+} ions released from nBG (Han et al., 2013) was observed and confirmed. Due to the presence of Ca^{2+} ions from nBG (even at a small amount of 0.1% (w/v)), there was a significant decrease (confirmed with one way ANOVA using the Bonferroni test for $p < 0.05$ = *, $p < 0.01$ = ** and $p < 0.001$ = ***) of strut size and an increase of pore size while keeping the printing pressure constant over 7 days. This effect indicates an improvement of the printing properties due the presence of nBG particles in the hydrogel ink.

Bertuola et al. (Bertuola et al., 2021) investigated the influence of BG (45S5 composition) content on the rheological parameters of a hydro-gel-based (gelatin–alginate–hyaluronic acid) ink. They reported a variation of viscosity in dependence of bioactive glass powder content, indicating the need to consider the interaction between the polymeric matrix and BG particles, which act like rigid fillers leading, in a certain concentration range, to an increase of viscosity. According to the results of this work, it is likely that with the incorporation of nBG particles the viscosity of alginate increases resulting in better printing fidelity. To confirm this assumption, further investigations in terms of rheology measurements of alginate hydrogels containing different concentrations of nBG particles should be performed in future.

3.3. Bioactivity of capsules

In order to assess the surface morphology of 1% (w/v) alginate capsules incorporating 0.1% (w/v) nBG particles before (day 0, reference) and after immersion in SBF for up to 28 days, SEM images were taken. SEM micrographs for the reference on day 0 (before immersion) and for days 14-28 are shown in Figure 3 and additional SEM images for days 1-7 are shown in Figure S4, Supplementary Information. To confirm the growth of HAp, FTIR spectra (Figure 4a) and XRD patterns (Figure 4b) were obtained. The formation of a HAp layer is a characteristic property of bioactive materials intended for bone tissue engineering or orthopaedic coatings (Kokubo & Takadama, 2006). The FTIR spectroscopy peaks of alginate capsules with nBG before and after 14-28 days of immersion in SBF are shown in Figure 4a. The infrared absorption of nBG usually occurs through vibrations of P-O and Si-O-Si bands (Filho, La Torre, & Hench, 1996). HAp $(Ca_{10}(PO_4)_6(OH)_2)$, exhibits FTIR absorption peaks due to hydroxyl groups (OH^-) and phosphate (PO_4^{3-}) vibrations. According
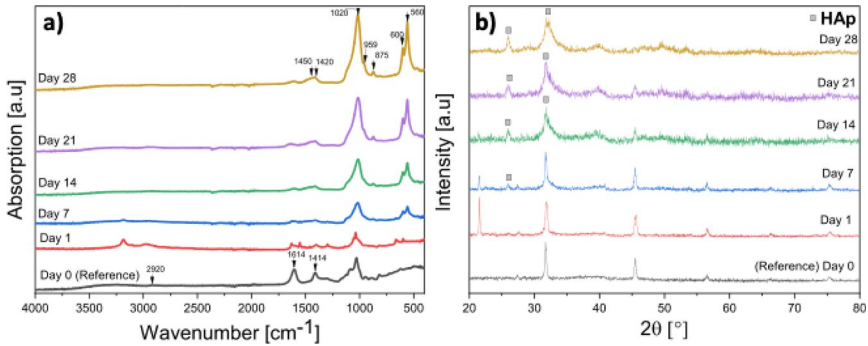
Figure 4. Formation of HAp layer on the surface of 1% (w/v) alginate capsules with 0.1% (w/v) nBG particles after 28 days immersion in SBF confirmed with a) FTIR spectra and b) XRD patterns.

Table 3. FTIR peaks assignment (see Figure 4a)).

Vibration mode	Wavenumber (cm⁻¹)	Refs.
Stretching of C-H	2920	(Papageorgiou et al., 2010)
Asymmetric stretching of COO⁻	1620–1610	(Mouriño et al., 2010)
Symmetric stretching of COO⁻	1430–1410	(Mouriño et al., 2010)
Stretching of PO_4^{3-}	1020	(Roguska et al., 2012)
HPO_4^{2-} ions	875, 959	(Roguska et al., 2012)
CO_3^{2-} vibration	875	(Roguska et al., 2012)
Bending of PO_4^{3-}	560, 600	(Roguska et al., 2012)

to the literature (Mouriño, Newby, & Boccaccini, 2010; Papageorgiou et al., 2010; Roguska et al., 2012) all identified adsorption peaks are summarized in Table 3. Due to stretching C-H vibration and stretching of symmetric and asymmetric COO⁻ groups the presence of alginate in the reference samples (before immersion in SBF) is confirmed. Even after 1 day of immersion two new small peaks ($550 \, cm^{-1}$ and $600 \, cm^{-1}$) appeared, which are ascribed to the bending vibration of PO_4^{3-}. A further peak appeared at $1020 \, cm^{-1}$, which can also indicate the formation of hydroxyapatite (Roguska et al., 2012). According to Roguska et al. (Roguska et al., 2012), the peaks at $875 \, cm^{-1}$ and $959 \, cm^{-1}$ may be an indicator of the presence of HPO_4^{2-}. Nevertheless, the detected peak at $875 \, cm^{-1}$ could indicate additionally a CO_3^{2-} group in carbonated hydroxy-apatite (Roguska et al., 2012). Therefore, it seems that HAp peaks overlap with the characteristic alginate peaks.

In addition to FTIR, XRD patterns were obtained to assess a possible phase change and to determine the formation of HAp. In Figure 4b the XRD patterns of the reference capsules with nBG (before immersion) and after immersion (day 1 and days 14-28) are shown. The formation of HAp on the surface of the capsules containing nBG

after immersion in SBF solution for up 28 days could be confirmed by XRD analysis. The main peaks at $2\theta = 26°$ and $2\theta = 32°$ indicate carbonated hydroxyapatite formation after 7-14 days (John, Hong, Ikada, & Tabata, 2001). An increase in the relative intensity of these two peaks could be observed with increasing immersion time in SBF. The limited formation of hydroxyapatite crystals may be explained through the relatively low volume fraction (0.1% (w/v)) of nBG and therefore a high amount of alginate hydrogel, which covered the surface of nBG particles and led to an inhibition of the contact of the particles with the SBF solution. Therefore, it can be concluded that after the degradation of alginate the capsules become 'more bioactive' (Nawaz et al., 2019). Furthermore, for non-immersed capsules crystalline peaks of combeite, with chemical structure $Na_2Ca_2Si_3O_9$, could be determined. According to literature, $Na_2Ca_2Si_3O_9$ is the main crystalline phase of sintered 45S5 BG and can therefore be ascribed to some crystalline content of the nBG used in this study (Chen, Thompson, & Boccaccini, 2006). Besides peaks indicating HAp, a slight decrease of crystalline peaks with an increase of immersion time was observed. The sharp peaks of combeite seem to decrease with an increase of soaking time in SBF solution and they finally disappear after 14 days. A possible reason for this phenomenon is that the remaining broad halo, which is created by a non-crystalline phase, overlaps with the HAp phase peaks. In addition, at least partial dissolution of nBG particles should be considered (Chen et al., 2006; Nawaz et al., 2019).

The surface morphology of capsules before immersion (day 0, reference) and after immersion (day 14-28) in SBF was additionally investigated by SEM, as shown in Figure 3. After 3 days of immersion in SBF the HAp formation on the surface of the capsules was observed. A clear morphology change of capsules in terms of the formation of a nanostructured layer and the formation of pores on the surface of alginate-nBG capsules was detected (Ur Rehman et al., 2017). Furthermore, an increasing size of this layer was observed, which indicates the growth of apatite crystals with increasing immersion time in SBF.

3.4. In vitro cell characterization

Figure 5a shows typical fluorescence images of 1% (w/v) alginate with and without nBG and 3% (w/v) alginate with and without nBG incorporating 1×10^6 cells/ml for days 0 and 7 (additional fluorescence images for days 1 and 3 are shown In Figure S5, Supplementary Information). Figure 5b shows the graphical evaluation of merged calcein
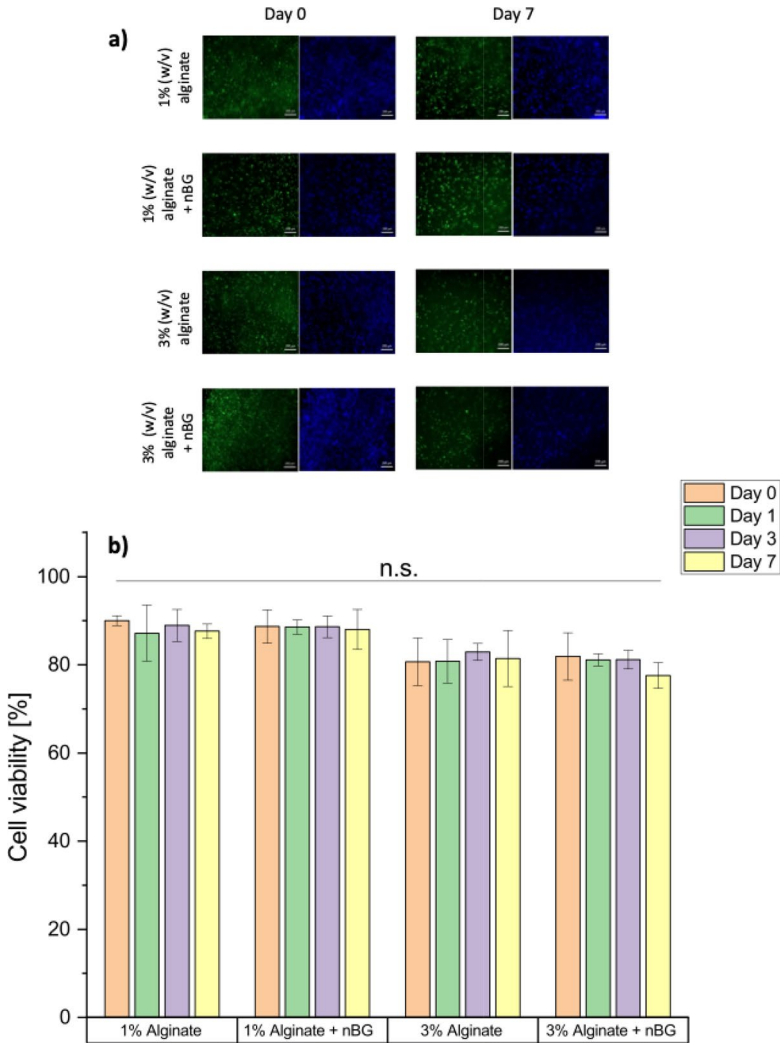
Figure 5. a) Fluorescence images of 1% and 3% (w/v) alginate bioinks with and without nBG, respectively, containing 1 x 10^6 cells/ml NIH/3T3 after 0 and 7 days of incubation, green: calcein, blue: DAPI. Scale bar: 200 µm. b) Cell viability of NIH/3T3 cells embedded in 4 bioinks: 1% (w/v) alginate with and without nBG particles and 3% (w/v) alginate with and without nBG particles over 7 days of incubation. Statistical analysis was performed via a one-way ANOVA with the Bonferroni test, n.s. = not significantly different.

(green) and DAPI (blue) images. The results indicate a high cell viability of all used bioinks during the printing study. Generally, calcein staining is used to investigate the intercellular esterase activity of living cells (Uggeri et al., 2004), whereas DAPI is used to stain the nucleus of cells

and therefore the total amount of cells (Tarnowski, Spinale, & Nicholson, 1991). After 7 days of incubation a high amount of viable cells for all 4 bioinks was found. After 7 days of incubation the cell viability for 1% (w/v) alginate was 89% ± 2, for 1% (w/v) alginate + 0.1% (w/v) nBG it was 88% ± 5, whereas for 3% (w/v) alginate it was around 81% ± 6 and for 3% (w/v) alginate + 0.1% (w/v) nBG it was 78% ± 3. It seems that the viability for 3% (w/v) alginate and 3% (w/v) alginate-nBG ink is slightly reduced after 7 days of incubation. This result could be due to the higher viscosity of alginate compared to 1% (w/v) alginate. Zhang et al. (Zhang et al., 2019) investigated the impact of different alginate concentrations on cell viability. Their results revealed a higher cell viability in low concentrated alginate inks in comparison to high concentrated alginate bioinks, which is in agreement with the present results. However, the results in the current study are not statistically significantly different. There is therefore no significant difference between pure alginate and alginate containing nBG inks, indicating that cell viability is not affected by nBG content. It seems that the relatively low nBG concentration of 0.1% (w/v) does not have a significant influence on the cell viability of NIH/3T3 cells over a time period of 7 days. A higher concentration should be investigated in further studies.

Moreover, a visual assessment of the calcein-DAPI images revealed an increasing density of cells with an increase in alginate concentration. A higher alginate concentration possesses more polymer chains which leads to an increased density of the ink, which can explain the higher cell density (Zhang et al., 2019).

Moreover, it seems that an increase of alginate concentration slightly reduces the viability of cells in the hydrogel. On the other hand, a higher concentration is necessary to provide a sufficient shape fidelity to create 3 D structures during the printing process. Therefore, a precise balance between high cell viability and stability of the printed 3 D structures must be considered. An increase of nBG concentration and therefore a higher Ca^{2+} concentration, which seems to lead to an increase of shape fidelity during the printing process, may solve the issue regarding finding the correct alginate concentration. However, an increase of nBG content can also have an impact on the hydrogel viability. Rottensteiner et al. (2014) incorporated 0.1% (w/v) 45S5 nBG particles into alginate dialdehyde (ADA)-gelatin (GEL) hydrogel. The addition of nBG showed a reduction of LDH and mitochondrial activity compared to pure ADA-GEL systems, which indicated an inhibition of cellular activity due to the presence of nBG (Rottensteiner et al., 2014). Therefore, the suggested increase of nBG and the associated impact on cell viability should be investigated in further studies.

4. Conclusions

In this study the impact of nBG particles on several properties of alginate hydrogels was investigated. A concentration of 0.1% (w/v) nBG and icariin as a drug model were used. nBG loaded alginate capsules were immersed in SBF to determine the bioactivity of capsules up to 28 days of immersion. The release study showed a significant impact of nBG particles on the release kinetics of icariin. Due to the presence of nBG and its associated Ca^{2+} ion release a decreased icariin release was achieved. Additional crosslinking of the hydrogel through Ca^{2+} ion release from nBG was inferred. During 3 D printing an improvement in terms of more precise grid sizes and associated pore sizes in nBG-alginate 3 D scaffolds was observed. In order to determine the bioactivity of nBG loaded alginate capsules, these were immersed in SBF. The formation of HAp layer on the surface of the capsules was confirmed by FTIR, XRD and SEM. Furthermore, to assess the cell viability of printed inks a calcein AM-DAPI staining was performed. A high cell viability for all used bioinks was observed.

Through the incorporation of nBG particles into alginate hydrogels, a significant improvement of alginate properties in terms of 3 D printed shape fidelity, improved icariin release ability and ability to develop an in vitro HAp layer in SBF was provided. Further investigations should consider variation/increase of the nBG concentration to assess the further impact on hydrogel properties. Overall, nBG incorporation into alginate matrices offers wide application in 3 D bioprinting and drug delivery approaches.

Disclosure statement

No potential conflict of interest was reported by the authors.

Funding

Notes on contributors

Faina Bider is a PhD student at the Institute of Biomaterials, University of Erlangen-Nuremberg. Her research focuses on composite hydrogels for biofabrication and drug delivery.

Emine Karakaya is a researcher at the Institute of Biomaterials, University of Erlangen-Nuremberg. Her expertise is the devolpment of alginate-based bioinks exhibiting promising cell-material interactions.

Dirk Mohn is a Research Associate at the University of Zurich and ETH Zurich. His expertise is in the development and application of bioactive glass for new medical devices within dental science.

Aldo R. Boccaccini is Professor of Materials Science (Biomaterials) and Head of the Institute of Biomaterials at University of Erlangen-Nuremberg, Germany. He works on bioactive and composite materials for tissue engineering and drug delivery.

References

Bajpai, S. K., & Sharma, S. (2004). Investigation of swelling/degradation behaviour of alginate beads crosslinked with Ca2+ and Ba2+ ions. *Reactive and Functional Polymers*, *59*(2), 129–140. https://doi.org/10.1016/j.reactfunctpolym.2004.01.002.

Banks, S. R., Enck, K., Wright, M., Opara, E. C., & Welker, M. E. (2019). Chemical modification of alginate for controlled oral drug delivery. *Journal of Agricultural and Food Chemistry*, *67*(37), 10481–10488. https://doi.org/10.1021/acs.jafc.9b01911.

Bertuola, M., Aráoz, B., Gilabert, U., Gonzalez-Wusener, A., Pérez-Recalde, M., Arregui, C. O., & Hermida, É. B. (2021). Gelatin–alginate–hyaluronic acid inks for 3D printing: Effects of bioglass addition on printability, rheology and scaffold tensile modulus. *Journal of Materials Science*, *56*(27), 15327–15343. https://doi.org/10.1007/s10853-021-06250-0.

Brunner, T. J., Grass, R. N., & Stark, W. J. (2006). Glass and bioglass nanopowders by flame synthesis. *Chemical Communications*, (13), 1384–1386. https://doi.org/10.1039/b517501a.

Cao, N., Fu, Y., & He, J. (2007). Mechanical properties of gelatin films crosslinked, respectively, by ferulic acid and tannin acid. *Food Hydrocolloids*, *21*(4), 575–584. https://doi.org/10.1016/j.foodhyd.2006.07.001.

Chen, F. M., & Liu, X. (2016). Advancing biomaterials of human origin for tissue engineering. *Progress in Polymer Science*, *53*, 86–168. https://doi.org/10.1016/j.progpolymsci.2015.02.004.

Chen, Q. Z., Thompson, I. D., & Boccaccini, A. R. (2006). 45S5 Bioglass-derived glass-ceramic scaffolds for bone tissue engineering. *Biomaterials*, *27*(11), 2414–2425. https://doi.org/10.1016/j.biomaterials.2005.11.025.

Draget, K. I., Skjåk-Braek, G., & Smidsrød, O. (1997). Alginate based new materials. *International Journal of Biological Macromolecules*, *21*(1–2), 47–55. https://doi.org/10.1016/S0141-8130(97)00040-8.

Filho, O. P., La Torre, G. P., & Hench, L. L. (1996). Effect of crystallization on apatite-layer formation of bioactive glass 45S5. *Journal of Biomedical Materials Research*, *30*(4), 509–514. https://doi.org/10.1002/(SICI)1097-4636(199604)30:4 < 509::AID-JBM9 > 3.0.CO;2-T.

Frampton, J. P., Hynd, M. R., Shuler, M. L., & Shain, W. (2011). Fabrication and optimization of alginate hydrogel constructs for use in 3D neural cell culture. *Biomedical Materials (Bristol, England)*, *6*(1), 015002–015018. https://doi.org/10.1088/1748-6041/6/1/015002.

Ghidoni, I., Chlapanidas, T., Bucco, M., Crovato, F., Marazzi, M., Vigo, D., … Faustini, M. (2008). Alginate cell encapsulation: New advances in reproduction and cartilage regenerative medicine. *Cytotechnology*, *58*(1), 49–56. https://doi.org/10.1007/s10616-008-9161-0.

Grassi, M., Colombo, I., & Lapasin, R. (2001). Experimental determination of the theophylline diffusion coefficient in swollen sodium-alginate membranes. *Journal of Controlled Release : Official Journal of the Controlled Release Society*, *76*(1–2), 93–105. https://doi.org/10.1016/S0168-3659(01)00424-2.

Han, Y., Zeng, Q., Li, H., & Chang, J. (2013). The calcium silicate/alginate composite: Preparation and evaluation of its behavior as bioactive injectable hydrogels. *Acta Biomaterialia*, *9*(11), 9107–9117. https://doi.org/10.1016/j.actbio.2013.06.022.

Jain, D., & Bar-Shalom, D. (2014). Alginate drug delivery systems: Application in context of pharmaceutical and biomedical research. *Drug Development and Industrial Pharmacy*, *40*(12), 1576–1584. https://doi.org/10.3109/03639045.2014.917657.

John, A., Hong, L., Ikada, Y., & Tabata, Y. (2001). A trial to prepare biodegradable collagen-hydroxyapatite composites for bone repair. *Journal of Biomaterials Science Polymer Edition*, *12*(6), 689–705. https://doi.org/10.1163/156856201316883485.

Khademhosseini, A., & Langer, R. (2016). A decade of progress in tissue engineering. *Nature Protocols*, *11*(10), 1775–1781. https://doi.org/10.1038/nprot.2016.123.

Khademhosseini, A., Vacanti, J. P., & Langer, R. (2009). Progress in tissue engineering. *Scientific American*, *300*(5), 64–71. https://doi.org/10.1038/scientificamerican0509-64.

Kokubo, T., & Takadama, H. (2006). How useful is SBF in predicting in vivo bone bioactivity? *Biomaterials*, *27*(15), 2907–2915. https://doi.org/10.1016/j.biomaterials.2006.01.017.

Kong, H. J., Lee, K. Y., & Mooney, D. J. (2002). Decoupling the dependence of rheological/mechanical properties of hydrogels from solids concentration. *Polymer (Polymer)*, *43*(23), 6239–6246. https://doi.org/10.1016/S0032-3861(02)00559-1.

Leite, A. J., Sarker, B., Zehnder, T., Silva, R., Mano, J. F., & Boccaccini, A. R. (2016). Bioplotting of a bioactive alginate dialdehyde-gelatin composite hydrogel containing bioactive glass nanoparticles. *Biofabrication*, *8*(3), 035005.

Mohn, D., Bruhin, C., Luechinger, N. A., Stark, W. J., Imfeld, T., & Zehnder, M. (2010). Composites made of flame-sprayed bioactive glass 45S5 and polymers: Bioactivity and immediate sealing properties. *International Endodontic Journal*, *43*(11), 1037–1046. https://doi.org/10.1111/j.1365-2591.2010.01772.x.

Mouriño, V., Newby, P., & Boccaccini, A. R. (2010). Preparation and characterization of gallium releasing 3-d alginate coated 45s5 bioglass® based scaffolds for bone tissue engineering. *Advanced Engineering Materials*, *12*(7), B283–291. https://doi.org/10.1002/adem.200980078.

Nawaz, Q., Ur Rehman, M. A., Roether, J. A., Yufei, L., Grünewald, A., Detsch, R., & Boccaccini, A. R. (2019). Bioactive glass based scaffolds incorporating gelatin/manganese doped mesoporous bioactive glass nanoparticle coating. *Ceramics International*, *45*(12), 14608–14613. https://doi.org/10.1016/j.ceramint.2019.04.179.

Orive, G., Carcaboso, A. M., Hernández, R. M., Gascón, A. R., & Pedraz, J. L. (2005). Biocompatibility evaluation of different alginates and alginate-based microcapsules. *Biomacromolecules*, 6(2), 927–931. https://doi.org/10.1021/bm049380x.

Ozbolat, I. T., & Hospodiuk, M. (2016). Current advances and future perspectives in extrusion-based bioprinting. *Biomaterials*, 76, 321–343. https://doi.org/10.1016/j.biomaterials.2015.10.076.

Papageorgiou, S. K., Kouvelos, E. P., Favvas, E. P., Sapalidis, A. A., Romanos, G. E., & Katsaros, F. K. (2010). Metal-carboxylate interactions in metal-alginate complexes studied with FTIR spectroscopy. *Carbohydrate Research*, 345(4), 469–473. https://doi.org/10.1016/j.carres.2009.12.010.

Rastin, H., Zhang, B., Mazinani, A., Hassan, K., Bi, J., Tung, T. T., & Losic, D. (2020). 3D bioprinting of cell-laden electroconductive MXene nanocomposite bioinks. *Nanoscale*, 12(30), 16069–16080. https://doi.org/10.1039/d0nr02581j.

Roguska, A., Pisarek, M., Andrzejczuk, M., Lewandowska, M., Kurzydlowski, K. J., & Janik-Czachor, M. (2012). Surface characterization of Ca-P/Ag/TiO2 nanotube composite layers on Ti intended for biomedical applications. *Journal of Biomedical Materials Research Part A*, 100(8), 1954–1962. https://doi.org/10.1002/jbm.a.34044.

Rottensteiner, U., Sarker, B., Heusinger, D., Dafinova, D., Rath, S. N., Beier, J. P., … Arkudas, A. (2014). In vitro and in vivo biocompatibility of alginate dialdehyde/gelatin hydrogels with and without nanoscaled bioactive glass for bone tissue engineering applications. *Materials (Basel, Switzerland)*, 7(3), 1957–1974. https://doi.org/10.3390/ma7031957.

Salgado, A. J., Coutinho, O. P., & Reis, R. L. (2004). Bone tissue engineering: State of the art and future trends. *Macromolecular Bioscience*, 4(8), 743–765. http://doi.org/10.1016/j.dental.2013.04.015.

Shen, X., Yu, P., Chen, H., Wang, J., Lu, B., Cai, X., … Li, Y. (2020). Icariin controlled release on a silk fibroin/mesoporous bioactive glass nanoparticles scaffold for promoting stem cell osteogenic differentiation. *RSC Advances*, 10(20), 12105–12112. https://doi.org/10.1002/mabi.200400026.

Tan, W. H., & Takeuchi, S. (2007). Monodisperse alginate hydrogel microbeads for cell encapsulation. *Advanced Materials*, 19(18), 2696–2701. https://doi.org/10.1039/d0ra00637h.

Tarnowski, B. I., Spinale, F. G., & Nicholson, J. H. (1991). DAPI as a useful stain for nuclear quantitation. *Biotechnic and Histochemistry*, 66(6), 296–302. https://doi.org/10.3109/10520299109109990.

Tønnesen, H. H., & Karlsen, J. (2002). Alginate in drug delivery systems. *Drug Development and Industrial Pharmacy*, 28(6), 621–630. https://doi.org/10.1081/DDC-120003853.

Tousi, N. S., Velten, M. F., Bishop, T. J., Leong, K. K., Barkhordar, N. S., Marshall, G. W., … Varanasi, V. G. (2013). Combinatorial effect of Si4+, Ca2+, and Mg2+ released from bioactive glasses on osteoblast osteocalcin expression and biomineralization. *Materials Science & Engineering C, Materials for Biological Applications*, 33(5), 2757–2765. https://doi.org/10.1016/j.msec.2013.02.044.

Uggeri, J., Gatti, R., Belletti, S., Scandroglio, R., Corradini, R., Rotoli, B. M., & Orlandini, G. (2004). Calcein-AM is a detector of intracellular oxidative activity. *Histochemistry and Cell Biology*, 122(5), 499–505. https://doi.org/10.1007/s00418-004-0712-y.

Ur Rehman, M. A., Ferraris, S., Goldmann, W. H., Perero, S., Bastan, F. E., Nawaz, Q., … Boccaccini, A. R. (2017). Antibacterial and bioactive coatings based on radio frequency co-sputtering of silver nanocluster-silica coatings on PEEK/bioactive glass layers obtained by electrophoretic deposition. *ACS Applied Materials & Interfaces*, *9*(38), 32489–32497. https://doi.org/10.1021/acsami.7b08646.

Vallet-Regí, M. (2006). Ordered mesoporous materials in the context of drug delivery systems and bone tissue engineering. *Chemistry (Weinheim an Der Bergstrasse, Germany)*, *12*(23), 5934–5943. https://doi.org/10.1002/chem.200600226.

Venkatesan, J., Bhatnagar, I., Manivasagan, P., Kang, K. H., & Kim, S. K. (2015). Alginate composites for bone tissue engineering: A review. *International Journal of Biological Macromolecules*, *72*, 269–281. https://doi.org/10.1016/j.ijbiomac.2014.07.008.

Wu, T., Nan, K., Chen, J., Jin, D., Jiang, S., Zhao, P., … Pei, G. (2009). A new bone repair scaffold combined with chitosan/hydroxyapatite and sustained releasing icariin. *Chinese Science Bulletin*, *54*(17), 2953–2961. https://doi.org/10.1007/s11434-009-0250-z.

Xynos, I. D., Edgar, A. J., Buttery, L. D. K., Hench, L. L., & Polak, J. M. (2001). Gene-expression profiling of human osteoblasts following treatment with the ionic products of Bioglass® 45S5 dissolution. *Journal of Biomedical Materials Research*, *55*(2), 151–157. https://doi.org/10.1002/1097-4636(200105)55:2<151::AID-JBM1001>3.0.CO;2-D.

Zeng, Q., Han, Y., Li, H., & Chang, J. (2014). Bioglass/alginate composite hydrogel beads as cell carriers for bone regeneration. *Journal of Biomedical Materials Research Part B, Applied Biomaterials*, *102*(1), 42–51. https://doi.org/10.1002/jbm.b.32978.

Zhang, X., Liu, T., Huang, Y., Wismeijer, D., & Liu, Y. (2014). Icariin: Does it have an osteoinductive potential for bone tissue engineering? *Phytotherapy Research : PTR*, *28*(4), 498–509. https://doi.org/10.1002/ptr.5027.

Zhang, J., Wehrle, E., Vetsch, J. R., Paul, G. R., Rubert, M., & Müller, R. (2019). Alginate dependent changes of physical properties in 3D bioprinted cell-laden porous scaffolds affect cell viability and cell morphology. *Biomedical Materials*, *14*(6), 065009. https://doi.org/10.1088/1748-605X/ab3c74.

Zhao, J., Ohba, S., Komiyama, Y., Shinkai, M., Il Chung, U., & Nagamune, T. (2010). Icariin: A potential osteoinductive compound for bone tissue engineering. *Tissue Engineering Part A*, *16*(1), 233–243. https://doi.org/10.1089/ten.tea.2009.0165.